Available online at www.sciencedirect.com
SCIENCE DIRECT
Polymer 47 (2006) 2133–2146
polymer
www.elsevier.com/locate/polymer

On significant retention of impact strength in clay–reinforced high-density polyethylene (HDPE) nanocomposites

M. Tanniru [a], Q. Yuan [a], R.D.K Misra [a,b,*]

[a] Center for Structural and Functional Materials, University of Louisiana at Lafayette, P.O. Box 44130, Lafayette, LA 70504-4130, USA
[b] Department of Chemical Engineering, University of Louisiana at Lafayette, P.O. Box 44130, Lafayette, LA 70504-4130, USA

Received 9 December 2005; received in revised form 14 January 2006; accepted 17 January 2006
Available online 7 February 2006

Abstract

The mechanical response of clay–reinforced polyethylene nanocomposite is investigated and the behavior compared with the un-reinforced polyethylene under identical conditions of processing. The micromechanism of plastic deformation during impact loading of neat polyethylene and clay–reinforced polyethylene nanocomposite are studied with scanning electron microscopy (SEM). The impact strength of composites is linked to structural studies by differential scanning calorimetry (DSC), dynamic mechanical analysis (DMA) and transmission electron microscopy (TEM) and SEM observations. The addition of clay to polyethylene retains adequately high-impact strength in the investigated temperature range of −40 to +70 °C. The micromechanism of deformation is altered from a combination of craze and drawing of fibrils in neat polyethylene to microvoid coalescence-fibrillated process in the nanocomposite. The aspects related to micromechanism of deformation are discussed.

Keywords: Plastic deformation; Microstructure; Polymer nanocomposites

1. Introduction

High-density polyethylene (HDPE) is considered a primary material in the materials substitution chain because of availability and recyclability. The performance criterion to encourage the application of HDPE requires superior modulus and yield strength in conjunction with high-impact strength. A substantial enhancement in mechanical properties (modulus, yield strength, and toughness) of thermoplastic materials can be realized by reinforcement with inorganic minerals including talc [1,2], mica [3], wollastonite [4–6], glass bead [7], and calcium carbonate [8–18].

In recent years, polymer nanocomposites have received significant attention, both in the industry and in academia during the past decade. They are a new class of multiphase materials containing dispersion of an ultra fine phase, typically in the range of 1–100 nm. They represent an attractive set of inorganic–organic materials (or organic–organic in some cases), not only from their obvious potential as technological materials, but also provide a convenient macroscopic system to study basic scientific issues concerning confined and tethered polymers at a new scale intermediate between the nano and microscale. A number of experimental investigations on these materials have indicated that polymer nanocomposites exhibit new and sometimes improved properties that are not displayed by the individual phases or by their conventional composite counterparts [19–28]. In polymer (polyethylene)–clay nanocomposite the clay particles are about the same size as the polymer molecules themselves, which enables them to be intimately mixed and chemically bonded to each other [29]. The improvement in mechanical properties such as tensile strength, tensile modulus [26–28,30–33], decreased thermal expansion coefficient, increased solvent resistance, outstanding diffusion barrier properties [23,24,34], and flame retardant capability [35,36] are a few selected examples of the advantages provided by this new class of materials. The presence of nanoparticles generally improves the elastic modulus, and does not significantly influence the rheological and processing behavior and the optical properties of the polymer matrix. It is presently believed that the local and global conformation of the polymers within the host galleries

* Corresponding author. Address: Center for Structural and Functional Materials, University of Louisiana at Lafayette, P.O. Box 44130, Lafayette, LA 70504-4130, USA. Tel.: +1 337 482 6430; fax: +1 337 482 1220.
E-mail address: dmisra@louisiana.edu (R.D.K. Misra).

0032-3861/$ - see front matter © 2006 Elsevier Ltd. All rights reserved.
doi:10.1016/j.polymer.2006.01.063

of nanoparticles are dramatically different from those observed in the bulk because of the confinement of the polymer chain and also due to specific polymer–surface interaction normally not observed in the bulk [34]. It is also believed that the local and chain dynamics are greatly affected by the confinement as well as the polymer–surface interactions. The basic reason for the synergistic improvement in properties is far from understood and the current thinking is that nanoparticle effects are related to optically confined polymer matrices, quantum size effects, and columbic-charging effects originating from ultra fine sizes, morphology, and interfacial interactions of the phases involved [37–39].

In clay–reinforced polymer nanocomposites, the significant increase in modulus is recognized and is reasonably understood. However, an understanding of the toughness behavior is still fragmented and less examined. The study of impact toughness is fundamentally important considering that the majority of semi-crystalline polymeric materials (polyethylene and polypropylene) are ductile at low-strain rates, but at high-strain rates such as those experienced in Izod impact test, exhibit a brittle behavior. Thus, the study of impact toughness at high-strain rates is of particular interest. Izod impact tests are also important because yield stress increases with strain rate, promoting brittle mode of fracture. Lastly, high-tensile toughness may not necessarily mean high-impact toughness.

The toughening behavior in polyvinylidene fluoride (PVDF) [40] and glassy polymer polylactide-*co*-glycolide (PLG) [41] by layered silicates nanoparticles (nanoclay) was recently examined by Giannelis group at Cornell via tensile tests. The significant enhancement in tensile elongation on reinforcement of PVDF with nanoclay was attributed to the reduction in spherulite size and the formation of the more mobile β-fiber-like crystallites. In the case of PLG–clay nanocomposites, crazing and shear yielding that require adequate mobility of polymer chain segments for plastic flow process contributed to greater percentage elongation-to-fracture of the nanocomposite. It was proposed that the polymer chains in the crazed zone were easily pulled into the fibrils of the craze, leading to extensive stretching of the fibrils. In contrast to the clay–reinforced nanocomposites, the enhancement of impact strength of calcium carbonate reinforced high-density polyethylene composites, where the rigid particles in comparison to clay are non-layered and nearly spherical was attributed by Tanniru and Misra [18] to the particle-induced cavitation and fibrillation. This process was encouraged by the amorphous nature of the particle–matrix interface. In comparison to crazing–tearing, the particle-induced cavitation process released plastic constraint and encouraged plastic deformation of the matrix.

In the present paper, impact on the toughness behavior of high-density polyethylene copolymer (PE)–4 wt% clay are described in terms of the response of the polymer matrix, in terms of nucleating capability of the reinforcement, crystal structure, percentage crystallinity, lamellae thickness, and matrix–particle interface.

2. Experimental procedure

2.1. Materials and physical properties

Commercially available grade of high-density polyethylene copolymer produced by Solvay (formal product name: ethane–hexene-1 copolymer) and developed for blow molding automotive fuel tanks and other large parts, where the finished part demands environmental stress crack resistance (ESCR), excellent processability and superior impact properties was used to process PE–4 wt% clay nanocomposites. This grade has a melt flow rate of 9 g/10 min at 190/2.16 kg. A natural montmorillonite clay surface modified with dimethyl dialkyl ammonium (Nanomer I.44P, Nanocor) was used as the reinforcement filler. The nanocomposites were prepared by mixing the appropriate amounts in twin screw extruder (counter rotating, 100 rpm) followed by injection molding of bars. The storage modulus of neat PE and PE–clay nanocomposites was studied by dynamic mechanical analysis (DMA). The DMA was carried out using TA instruments 2980 in single cantilever mode from −125 to 120 °C. The testing frequency was 1 Hz and the heating rate was 3 °C/min.

2.2. Crystallization behavior, structural characteristics, and dispersibility

The study of degree of crystallinity assumes particular significance because higher crystallinity, in general, increases modulus and yield stress, and reduces toughness. The change in percentage crystallinity, and structural characteristics induced by clay is important in understanding the deformation behavior. The crystallization behavior of neat PE and clay–reinforced PE nanocomposites was studied by differential scanning calorimetry (DSC). The PE and PE–clay nanocomposites were heated from room temperature (∼20 °C) to 200 °C and held at the high temperature for about 3 min in order to erase the previous thermomechanical history and to obtain a completely relaxed melt. Then the melt was cooled to 30 °C at the rate of 10 °C/min, and a second scan was carried out at the rate of 10 °C/min.

The dispersibility and intercalation of PE into the clay layers was studied by transmission electron microscopy (TEM). The staining was carried out in the vapor phase. The trimmed specimen was stained by staying with solid ruthenium tetroxide (RuO_4) for 10 h in a vial [42]. Sections of 100–200 nm were cut using a Leica ultramicrotome equipped with a diamond knife and collected in a trough filled with water and placed directly on 400-mesh copper grids. Transmission electron micrographs were taken with Hitachi H-7600 at an acceleration voltage of 100 kV.

2.3. Mechanical properties

The tensile bars of neat and PE–clay nanocomposites were tested in uniaxial tension at 20 °C using a computerized MTS 210 tensile testing machine at selected displacement rate of

~5 mm/min to determine tensile properties (modulus, yield strength) in accordance with ASTM D-638. The Izod impact tests were carried out using an instrumented falling weight Tinius Olsen impact tester (Model 899) with an impact velocity of 1 m/s. The notched specimens were subjected to the impact test in the temperature range of −40 to +70 °C.

The fracture surface of Izod impact tested specimens as a function of temperature was studied using field emission SEM (JEOL 6300F) after coating with gold to minimize electrostatic charging.

2.4. Morphological characterization

The fracture surface of Izod impact tested specimens at −40 °C was studied using field emission SEM (JEOL 6300F) after coating with gold to minimize electrostatic charging. The surface morphology of isothermal crystallized samples (120 °C) of both neat PE and PE–4 wt% clay nanocomposite was observed using SEM after etching with potassium permanganate.

3. Results and discussion

3.1. Crystallization and structural characteristics

The DSC plots for neat PE and PE–4 wt% clay are presented in Fig. 1 and the crystallization data (percentage crystallinity, melting and crystallization temperatures) summarized in Table 1. The percentage crystallinity was estimated using a value of heat of fusion of 293 J/g [43]. The crystallinity increases with the addition of clay from 39.8 to 56.1%, but the crystallization temperature remains unaffected. In our recent study of PP–clay nanocomposites, both the crystallinity and crystallization temperature of polymer nanocomposite increased, this was attributed to the nucleation role of clay. In present case, the increase in crystallinity can be ascribed to the nucleating effect of nanoclay, while the reason for crystallization temperature of PE–clay nanocomposite remaining unaltered may be related to the particle–matrix interaction, as discussed later in Section 3.5.3. The interfacial interaction plays a critical role in the free energy of cluster formation and the rate of nucleation; the weak interaction lowers the rate of nucleation. The DMA results also indicated weaker interaction between PE matrix and nanoclay, compared with polypropylene–clay nanocomposite (Section 3.5.3). Also, listed in

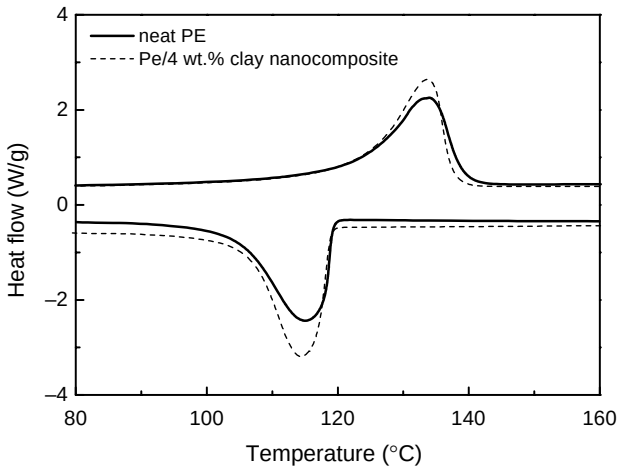

Fig. 1. Differential scanning calorimetry plots for neat PE copolymer and 4 wt% clay–reinforced PE copolymer nanocomposite.

Table 1 are lamellar thickness (l). The lamellar thickness is given by the Thomson–Gibbs equation [44]

$$l = \frac{2\gamma T_m^0}{(\Delta H \rho (T_m^0 - T_m))} \quad (1)$$

where T_m^0 is the equilibrium melting temperature, T_m is the detected melting temperature by DSC, γ the surface free energy, ΔH the heat of fusion for 100% crystalline polyethylene, and the density. The slightly increase in melting temperature is correlated to the slightly increase in lamellae thickness and indicates the perfection of crystals improved with the addition of clay particles.

Representative SEM micrographs of the crystal structure of 120 °C crystallized neat PE and PE–4 wt% clay nanocomposite are presented in Fig. 2. It is found that the addition of clay slightly affects the crystal structure (shape and size) of the matrix polymer by making it finer.

3.2. Dispersion and intercalation of clay

The dispersion of clay nanoparticles in the nanocomposite is presented in Fig. 3(a). The particles are uniformly distributed in the matrix and do not give an indication of aggregation. Uniform dispersion is important because in case of a matrix with aggregates of particles, the stress field will be concentrated around any aggregates, such that the cracks will propagate easily

Table 1
Physical and mechanical properties of high-density polyethylene copolymer and clay reinforced–PE copolymer nanocomposites

Material	Heat of fusion for polyethylene (J/g)	% Crystallinity DSC	Crystallization temperature (°C)	Melting temperature (°C)	Lamellae thickness (nm)	Glass transition temperature (°C)	Modulus at 5 mm/min (MPa)	Yield stress at 5 mm/min (MPa)	Elongation at break (%)
Neat PE	116.2	39.8	115.0	133.3	7.72	−114.1	606.3	23.9	800
4 wt% clay–PE nanocomposite[a]	147.4	56.1	114.4	113.7	7.79	−116.2	767.0	24.6	362

[a] For 100% polyethylene.

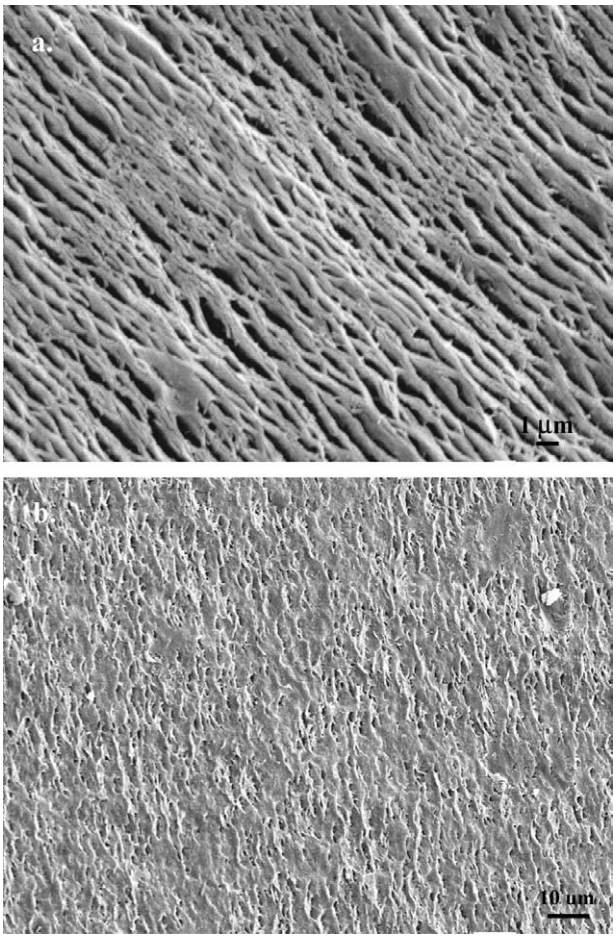

Fig. 2. Scanning electron micrographs of etched neat PE copolymer and 4 wt% clay–reinforced PE copolymer nanocomposite crystallized at 120 °C. (a) Neat PE and (b) 4 wt% clay–reinforced PE copolymer nanocomposite.

and rapidly, causing premature failure. The higher magnification TEM micrograph (Fig. 3(b)) shows the intercalation of clay. Furthermore, it is also interesting to note that crystalline lamellae parallel to the clay layers (Fig. 3(b1)) and are present between the intercalated galleries of clay (Fig. 3(b2)). The existence of parallel lamellae in the vicinity of the clay makes us to believe that interphase around the particle is a characteristic of the crystalline nature of the particle–matrix interface.

3.3. Mechanical properties

The tensile modulus and yield stress data are listed in Table 1. The data in Table 1 also includes data for 4 wt% clay–reinforced polyethylene. The elastic modulus increased from 606.3 MPa in neat polyethylene to 767.0 MPa in 4 wt% clay nanocomposite. However, the yield stress remained unaffected because of weak interaction between filler and the polymer matrix. A similar behavior was observed for wollastonite- [6] and talc-reinforced [1,2] polypropylenes and ethylene–propylene copolymers [45]. This is discussed below.

The previous work [46] indicated that an increase in crystallinity or increase in spherulite size increases the modulus because large spherulites are considered to exhibit significantly higher load-bearing capability. However, in the present study, there is increase in crystallinity but the crystal structure remains unaffected (Fig. 2) on reinforcement with clay nanoparticles. The observed significant increase in crystallinity is most likely to be because of higher nucleation density induced by the clay particles. To rationalize these observations, it is appropriate to say that the reinforcement of polyethylene with consequent increase in percentage crystallinity increases the modulus of nanocomposites. In summary, it is the reinforcement effect that dominates the mechanical behavior. Friedrich [47] first emphasized the effect of morphology and provided evidence that semi-crystalline polymers consisting of small spherulites are generally tougher than those containing coarse spherulites because larger spherulites have weak boundaries. Friedrich's conclusion [47] was confirmed by Ouderni and Philips [48] from their study on the effect of crystallinity. It was observed that an increase in crystallinity or spherulite size decreased the toughness.

The above observations of Friedrich [47] and Ouderni and Philips [48] do not appear to be applicable for the composites. In our case, there is increase in crystallinity, which according to the observations of Friedrich [47] and Ouderni and Philips [48] should have a negative effect on toughness. Thus, the observations made here suggests that the behavior of the composite is not a simple function of crystallinity and crystal structure (morphology), but is a complex function of other factors and includes lamellar thickness and interfacial interaction. Table 1 shows that the lamellar thickness was slight increased with percentage clay reinforcement. The lamellar thickness is an important controlling parameter in the activation of yield, and yield stress in neat semi-crystalline polymers is proportional to lamellar thickness [49]. As a result, the reinforcement effect of clay with consequent increase in percentage crystallinity increases the modulus of the composite.

3.4. Izod impact toughness

Izod impact strength for PE and PE–4 wt% clay nanocomposite are presented in Fig. 4 for tests conducted in the temperature range of −40 to +70 °C. It may be noted that the addition of clay to PE though decreases the impact strength for the entire temperature range of Izod impact tests, however, the toughness continues to be high even at −40 °C (10 kJ/m^2).

3.5. Fractography

The examination of fracture surface at −40 °C reveals strikingly different features and fracture zones in neat PE (Figs. 5 and 6) and PE–clay nanocomposite (Figs. 7 and 8). Macroscopically, the fracture surface appeared highly ductile in neat PE (Fig. 5) and less ductile or brittle-like in PE–clay nanocomposite (Fig. 7). This macroscopic difference suggests that the crack propagation occurred at a rapid rate in the

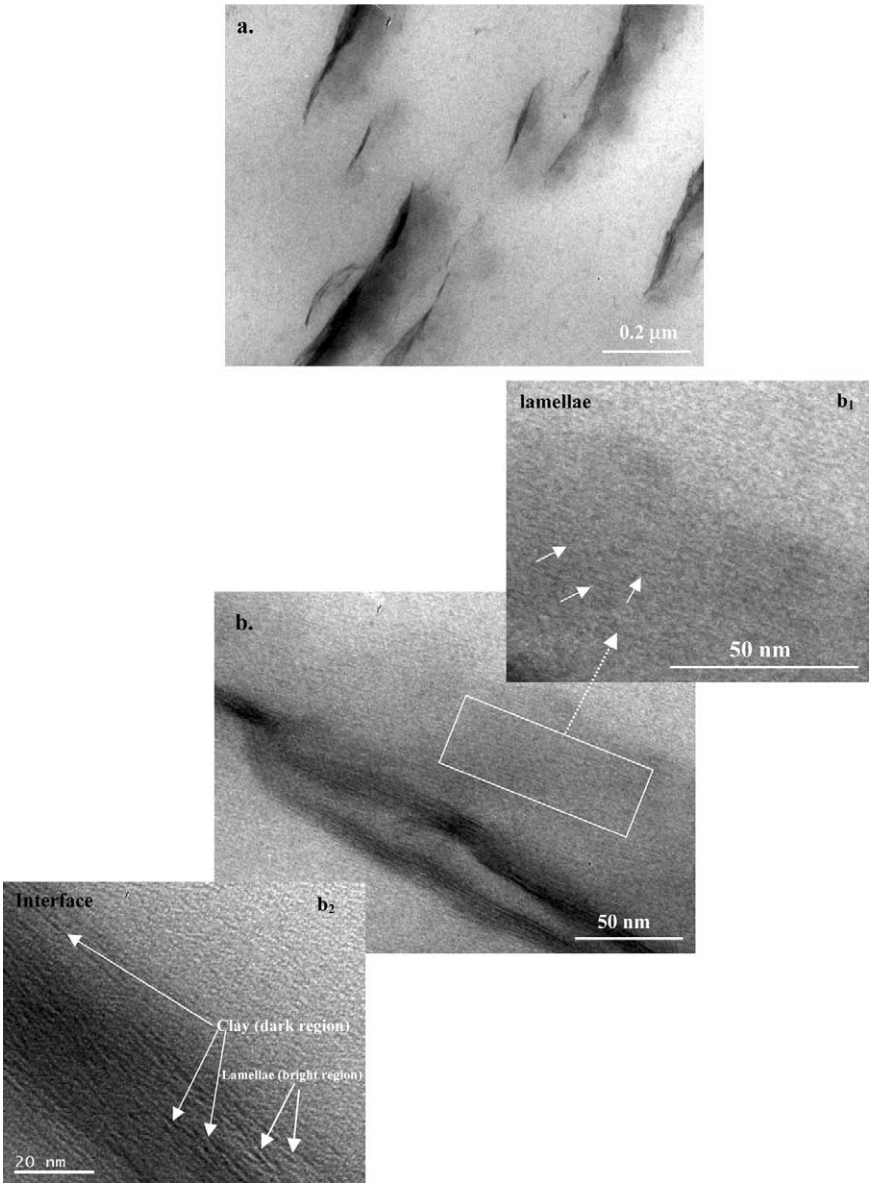

Fig. 3. Transition electron micrographs showing (a) uniform distribution of clay and (b) intercalation of clay in PE copolymer nanocomposite.

nanocomposite. We shall first describe the fracture characteristics of neat PE copolymer.

3.5.1. Fracture characteristics of neat polyethylene

The macroscopic fracture surface of neat PE impacted tested at −40 °C is presented in Fig. 5 and is clearly indicative of a highly ductile mode of fracture. From Fig. 5, two primary zones can be defined and include initiation zone (zone 1) and the crack propagation zone (zone 2) (Fig. 5(a)–(c)). Both the initiation and propagation zones can be further subclassified. Initiation zone consists of zones 1A and B. The zone 1A resembles a craze-like region with large vein-type features involving tearing of the material (Fig. 5(c)). Within the shallow vein-type features, extensive drawing of fibrils can be seen implying considerable degree of plastic deformation (Fig. 5(d)). Ahead of zone 1A, is zone 1B, characterized by a

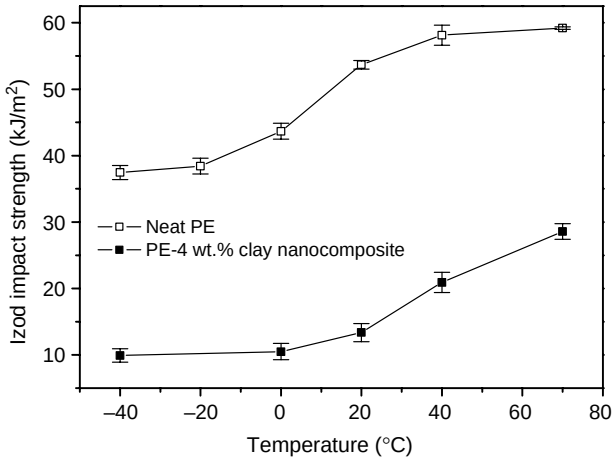

Fig. 4. Izod impact strength for neat PE copolymer and 4 wt% clay–reinforced PE copolymer nanocomposite as a function of temperature.

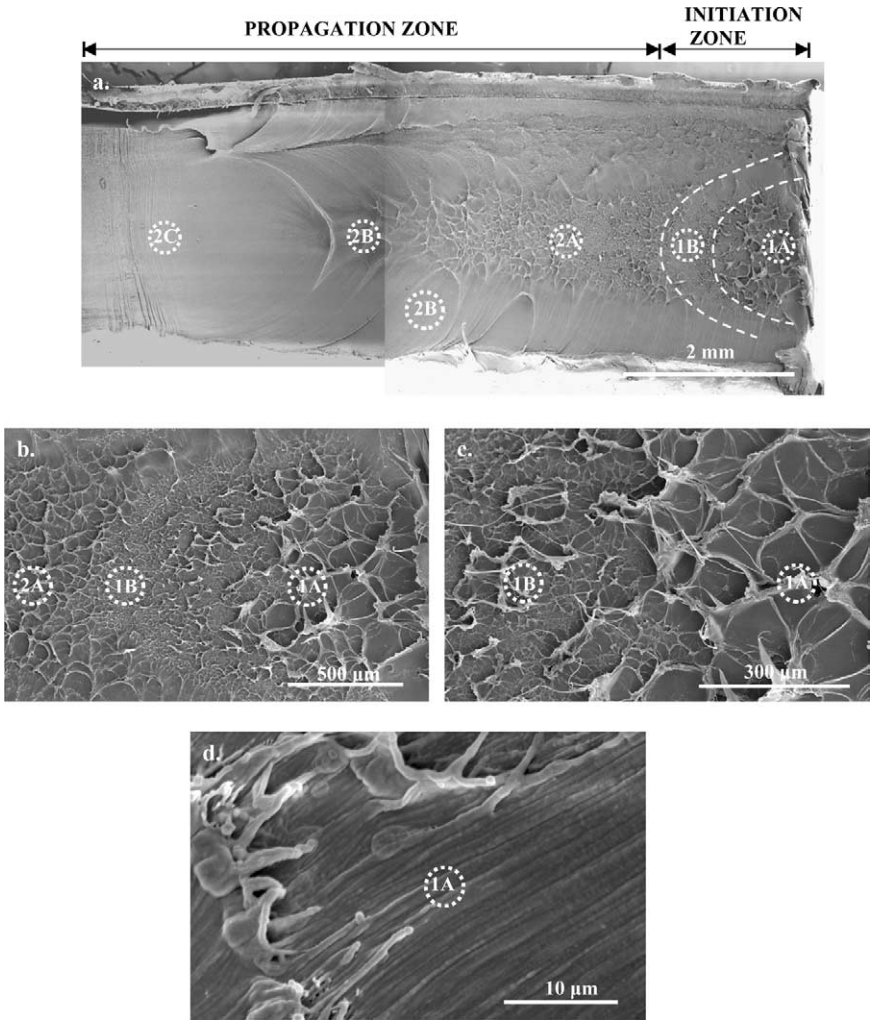

Fig. 5. Scanning electron micrographs of the fracture surface of neat PE copolymer showing initiation (zone 1A, craze-like zone; zone 1B, less ductile zone) and different propagation zone (zone 2A, craze-like zone; zone 2B, less brittle-like zone) at different magnifications.

less ductile zone with small shallow features (Fig. 5(e) and (f)). In zone 1B, the drawing of fibrils is significantly less (Fig. 5(f)). The high toughness of PE results in slower breakdown of the initiation zone and is characterized by a initial propagation zone 2A (Fig. 5(a), (g) and (h)), followed by zones 2B and 2C. The zone 2A at high-magnification images (Fig. 5(g) and (h)) is similar to zone 1A. An important characteristic feature of the fracture surface is the formation of parabolic or conical markings in zone 2B (Fig. 5(a) and (i)), ahead of the propagation zone 2A. The fracture morphology observed at the edge of the sample in zones 1A, 1B, and 2A (Fig. 5(a)) was similar to zone 2B (Fig. 5(a)). It is envisaged that the growth and propagation of the macroscopic crack is accompanied by nucleation of secondary 'plastic' microcracks ahead and on the sides of the primary macroscopic crack (notch) at a local region of heterogeneity, as depicted in Fig. 6. An example of a nucleation site and outward growth is presented in Fig. 5(i)–(k) and the magnified view of the parabolic region marked with a box is shown in Fig. 5(l) and (m). Another example of the nucleation point emanating in the vicinity of the edge of the sample and growing inwards to the center is presented in Fig. 5(n) and (o). The primary crack and the new secondary microcracks grow and eventually interact such that the locus of interaction of the main crack front and the microcracks is the parabola (Fig. 6). In the high-magnification view of the parabolic markings, a secondary detail in the form of fine striations or fibrillation is clearly visible (Fig. 5(l) and (m)). The striations or fibrils are parallel to the local direction of the crack growth and are result of severe plastic deformation processes. When the microcracks are nucleated out of the plane of the main crack, the microcracks overlap each other, as schematically shown in Fig. 7. The final fracture occurs when overlapping primary and secondary cracks bow out and river-like steps at the scale of nanometer develop within the highly deformed polymer matrix, as identified in Fig. 5(m). The last stage of propagation, zone 2C, was characterized by stop–go-events. The crack fronts were well defined indicating that some irreversible deformation occurred at the propagating crack tip leaving residual markings on the fracture surface Fig. 5(a). With increase in temperature up to +70 °C, the extent of the craze-like zone (zone 1A, zone 1B) was reduced. A schematic representative is shown in Fig. 6.

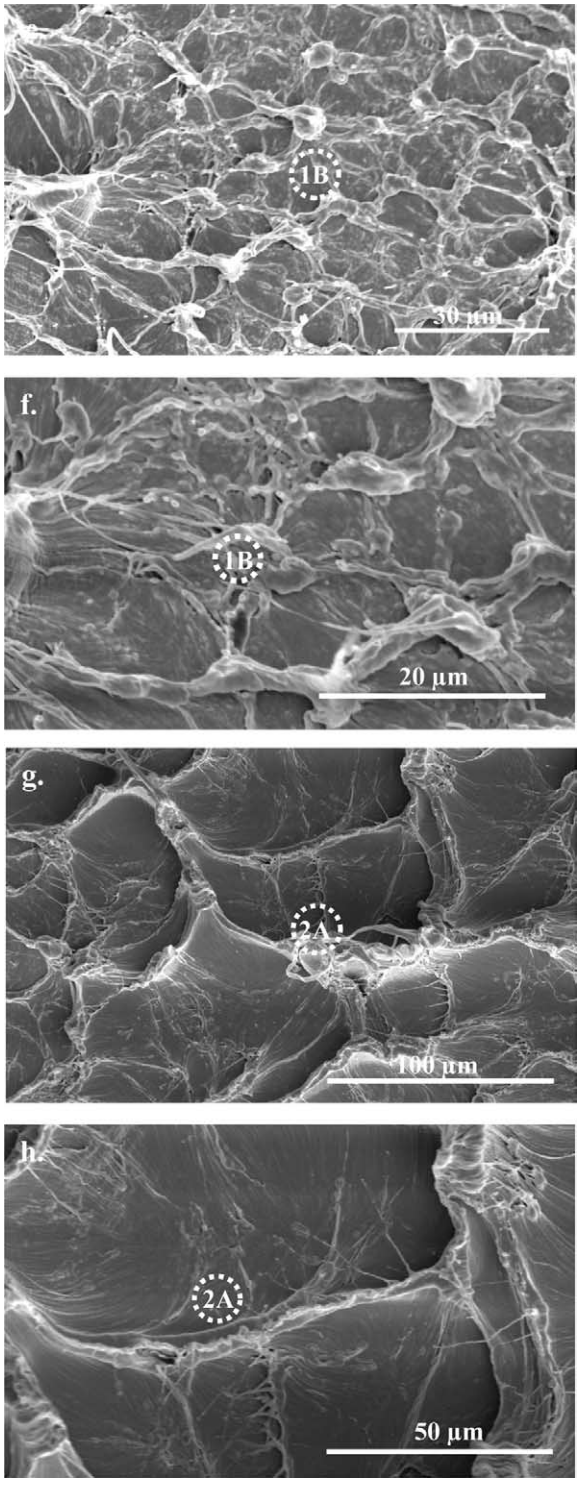

Fig. 5 (*continued*)

3.5.2. Fracture characteristics of clay–reinforced polyethylene

In contrast to neat polyethylene, the overall macroscopic fracture surface behavior of PE–clay nanocomposite at −40 °C appears brittle-like and rougher with seemingly little macroscopic plastic deformation before fracture but as described below the fracture process involved extensive plastic deformation in different zones (Fig. 8(a)). We can define two primary zones, initiation (zone 1) and propagation zones (zone 2). The nature of the fracture surface morphology in the two zones was different from neat PE copolymer. In general, the characteristics of the fracture surface were similar at all test temperatures except for the extent of the individual zones. The macroscopic and microscopic features are presented in Fig. 8.

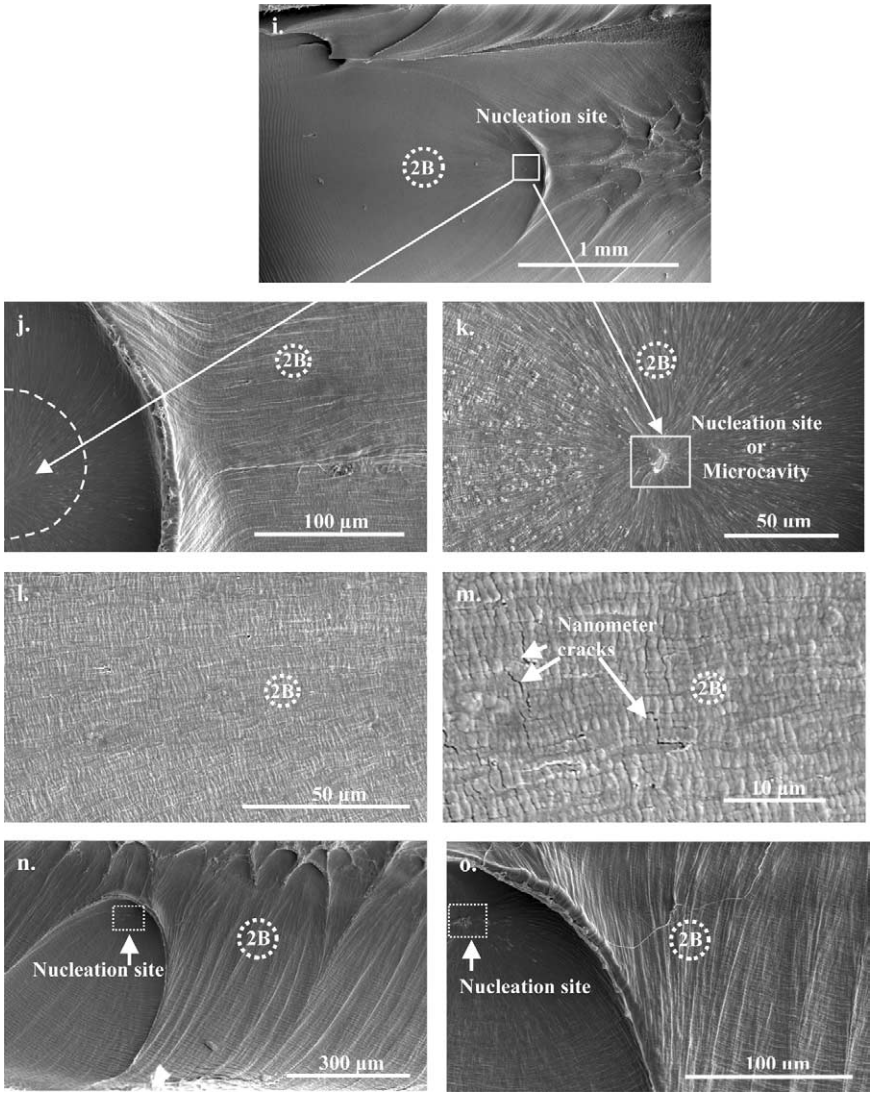

Fig. 5 (*continued*)

The crack initiation zone has two small subzones (zones 1A and B) with significant differences in the ductile morphology. In a manner similar to neat PE, the first subfracture initiation zone (zone 1A) was characterized by a craze-like ductile zone (Fig. 8(b)) with tearing leading to large shallow features of size 100–200 μm (zone 1A) (Fig. 8). The elongated fibrils here are much finer implying considerable amount of plastic deformation but significantly less dense, when compared with zone 1A in neat PE. At high magnification, zone 1A is ductile involving microvoids and extensively deformed fibrils (fibrillation) (Fig. 8(d)). The combination of microvoid coalescence and fibrillated appearance results from the nucleation and growth of a large number of microvoids and extensive localized deformation of ligaments between the microvoids. The microvoids later on coalesce and the crack propagates unstably. Even in the impact test, the elements of the material or ligaments between the microvoids draw down to fine points, before separation of polymer molecules past each other occur, producing fibrillated fracture. The highly stretched material then shrinks producing an appearance presented in the high-magnification image of zone 1A in Fig. 8(e). The combination of microvoid and fibrillated fracture can be understood in terms of two interactive processes. First, the nucleation of microvoids in the vicinity of particles provides stress concentration centers that determine the density of microvoids. Second, the viscoelastic plastic processes associated with the growth of microvoids and the deformation of ligaments bridging the microvoids. The ligaments or islands of material between the microvoids must fracture before the final separation occurs. An explanation for the mechanics of fracture necessitates a model that can predict the nucleation, density, and growth of microvoids, all of which are dependent on the state of stress. We are currently examining this aspect. A schematic of the envisaged microvoid coalescence-fibrillated fracture process is presented in Fig. 9. The initiation zone 1A is dominated by microvoid coalescence. This may suggest that the ability of

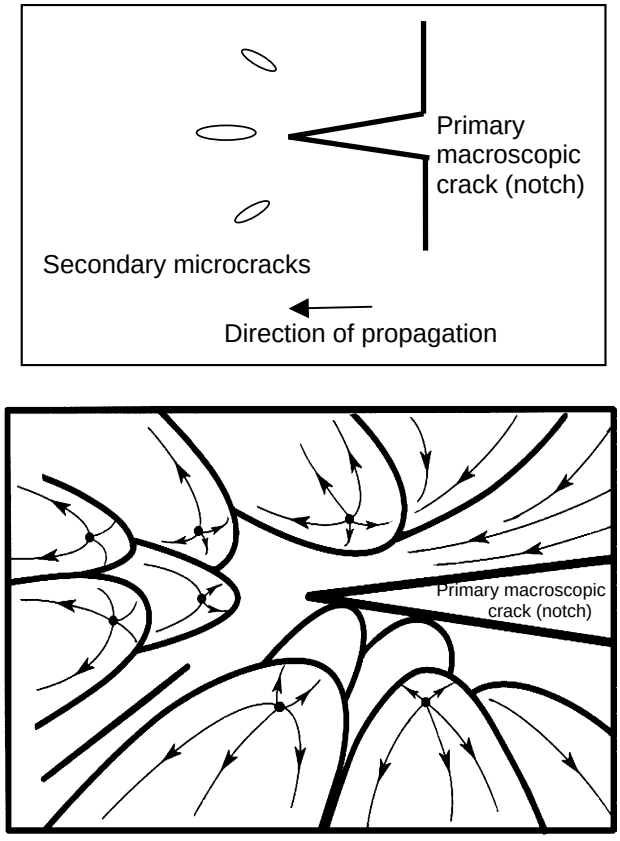

Fig. 6. Schematic of growth and propagation of the macroscopic crack in zones 1 and 2 of Fig. 5.

the material to experience high-ductile behavior, but the higher crystallinity and reinforcement clay offers resistance to plastic deformation. The reduced density of fibrils/fibrous structure implies lower amount of energy is absorbed in clay–reinforced PE copolymer. The formation of dense fibrils in PE copolymer must be responsible for the observed significantly high toughness in relation to the nanocomposite. On the other hand, the reduced density of fibrils in the nanocomposite suggests formation of greater number of shallow microvoids and dimpled pattern. The second initiation zone 1B (Fig. 8(e) and (f)) has reduced ductility in relation to zone 1A.

The rapid breakdown of the craze initiation zone does not provide adequate time for the material ahead of the initiation zone 1A to respond such that a second smooth region 1B surrounds the zone 1A. The second initiation zone (zone 1B) has reduced ductility in relation to zone 1A.

The propagation zone 2 with brittle-like appearance (Fig. 8(a)) also involved microvoid coalesence (Fig. 8(h) and (i)) in a manner similar to zone 1A, but with reduced plasticity. A schematic of the relative extent of different zones is summarized in Fig. 10. The zone was observed to decrease with increase in temperature with consequent increase in the shear-lip propagation zone (zone 2B). In general, the fracture surface of PE copolymer–4 wt% clay nanocomposite was predominantly characterized by microvoid and fibrillation, with fibrillation being significantly being less in zone 1B.

3.5.3. Toughness of clay–reinforced polyethylene copolymer nanocomposites

It is clear from the relative comparison of the initiation and propagation zone in neat PE copolymer and PE–4 wt% clay nanocomposite that the reinforcement leads to transformation of the fracture surface from predominantly dense fibrous structure to predominantly microvoid coalescence fracture. In both neat PE copolymer and in the nanocomposite, the fibrils in the initiation craze zone have the ability to significantly plastically deform before fracture, except that in the nanocomposite, the ability is reduced. Thus, it is believed that clay must be the source of microvoid nucleation. The matrix ligaments between these voids are extensively deformed in the propagation zone leading to a combination of microvoid coalescence and fibrillated fracture. In general, both the initiation and propagation zones exhibit various degrees of ductility, where small size microvoids and severely deformed fibrils are indicative of higher microplasticity.

If we compare similar magnification Figs. 5(d) and 8(i) for PE copolymer and nanocomposites, respectively, it may be noted that the fibrous structure is highly dense with no apparent large size microvoids in PE copolymer. On the other hand, in the nanocomposite, the density of fibrils is dramatically reduced but significant plastic deformation of a few stretched fibrils can be seen. But the fact that toughness is reduced and densely populated fibrous structure is not observed in the nanocomposite implies that some structural features of the

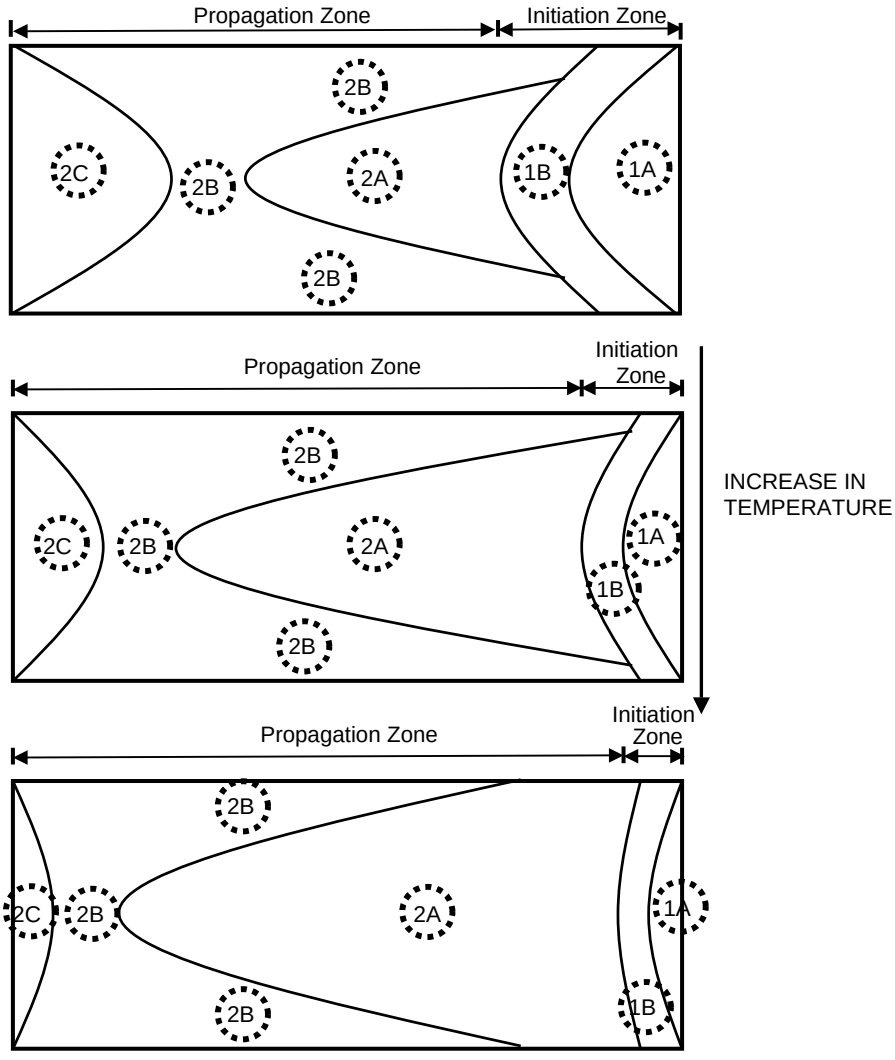

Fig. 7. Schematic of the extent of initiation and propagation zones as a function of temperature in neat PE copolymer.

nanocomposite offer resistance to plastic deformation. It may be noted that our recent work on polypropylene–4 wt% clay nanocomposites processed under identical conditions indicated an increase in toughness in the temperature range of −40 to +70 °C. From DSC results (Table 1), the crystallization temperature of PE–clay nanocomposite remains almost same with the addition of clay. While in polypropylene–clay nanocomposites, the crystallization temperature of polypropylene increased over 15 °C. This implies that the nucleating effect of clay in PE–clay nanocomposites is less obvious than that in polypropylene–clay nanocomposites. On the other hand, from the DMA results (Fig. 11) it can be observed that the tan δ peak of the nanocomposite (glass transition temperature, T_g) shifts only slightly to lower temperature on reinforcement with clay (Table 1). This can be explained in terms of the weak interaction between nanoclay particles and the PE matrix. In addition, the storage modulus of the nanocomposite remains unaffected on the addition of clay. Comparing with polypropylene–clay nanocomposite system, the reason why the addition of clay to PE decreases the impact strength for the entire temperature range of Izod impact tests maybe ascribed to the interaction between nanoclay particles and polymer matrix. During mechanical deformation, the relative weak part (particle–filler interface) though believed to be crystalline from Fig. 3, is first to deform.

The toughness of a material is generally related to the energy dissipating events that occur in the vicinity of a sharp crack. In HDPE copolymer, the highly dense fibrous structure is responsible for high toughness and the final fracture occurs due to nanoscale cracks formed between the stretched fibrils, as arrowed in Fig. 5(m). While in the nanocomposite, the microvoids nucleated due to clay releasing the plastic constraint in the matrix, triggering large scale plastic deformation with consequent tearing of matrix ligaments between microvoids resulting in stretching of fibrils (fibrillation) interdispersed with microvoids (Fig. 8(h) and (i)). Each of the above outlined processes, fibrillation, or microvoiding, and matrix yielding contribute to energy absorption [10,17]. Thus, there is a clear relationship between the fracture mode and impact strength of neat HDPE copolymer and clay–reinforced

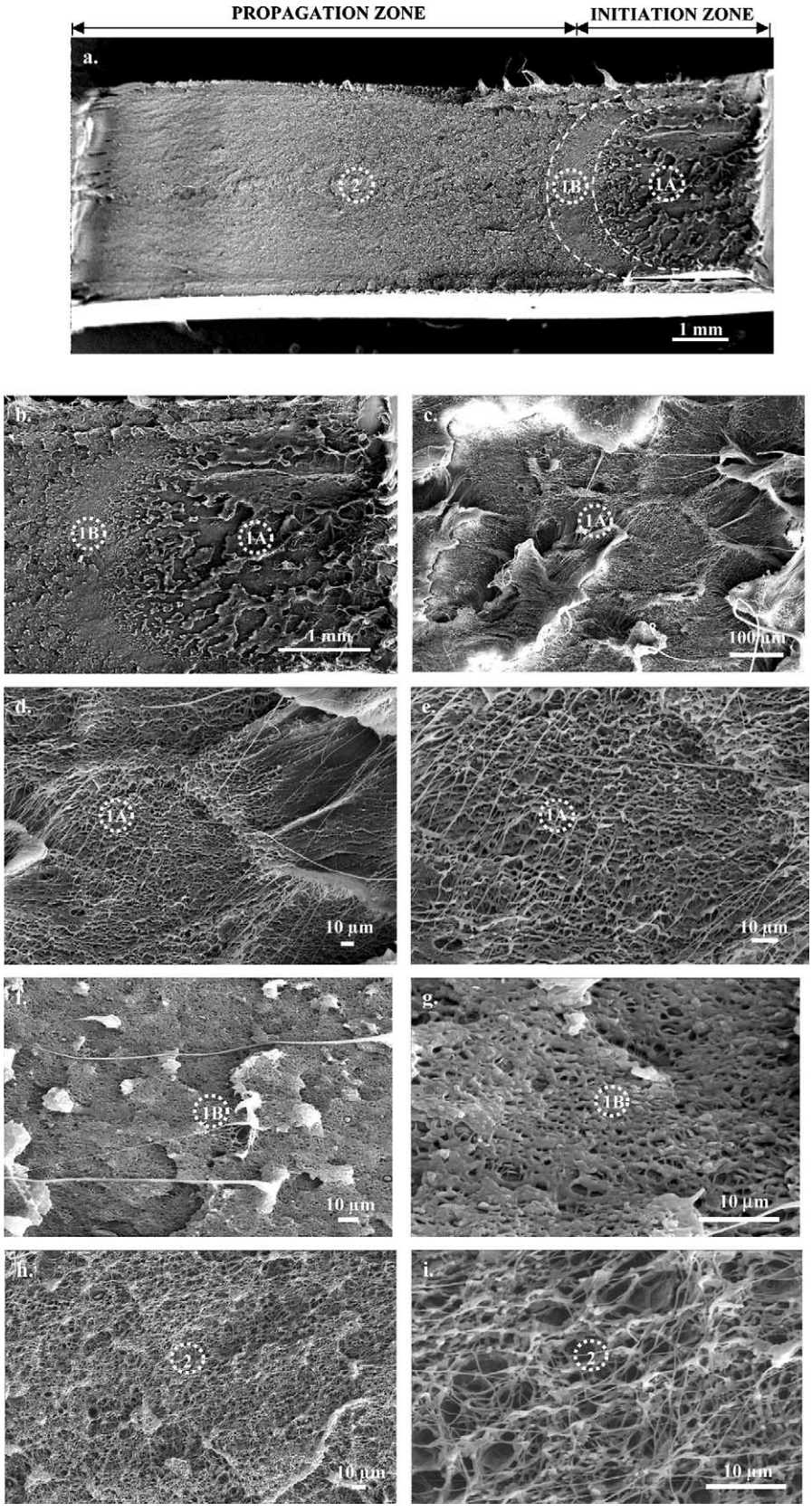

Fig. 8. Scanning electron micrographs of the fracture surface of PE copolymer nanocomposite showing initiation (zones 1A and B) and propagation zone (zone 2). Similar behavior was observed at other temperatures.

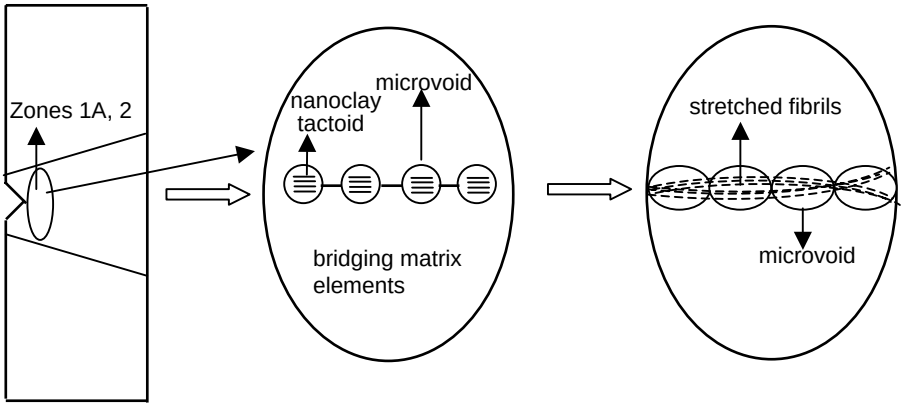

Fig. 9. Schematic of the envisaged microvoid coalescence-fibrillated fracture process operative in PE–clay nanocomposite.

nanocomposites. The observations made here are consistent with fractography observations made in tensile strained HDPE copolymer and HDPE–clay nanocomposites [17].

In mineral-reinforced semi-crystalline thermoplastic materials, the microdeformation processes identified as energy dissipating mechanisms include crazing, cavitation or debonding of minerals with consequent microvoid formation, deformation bands and fibrillation [1,6,7,10,50–58]. The occurrence of the above outlined microdeformation process is, however, governed by the structural characteristics of the

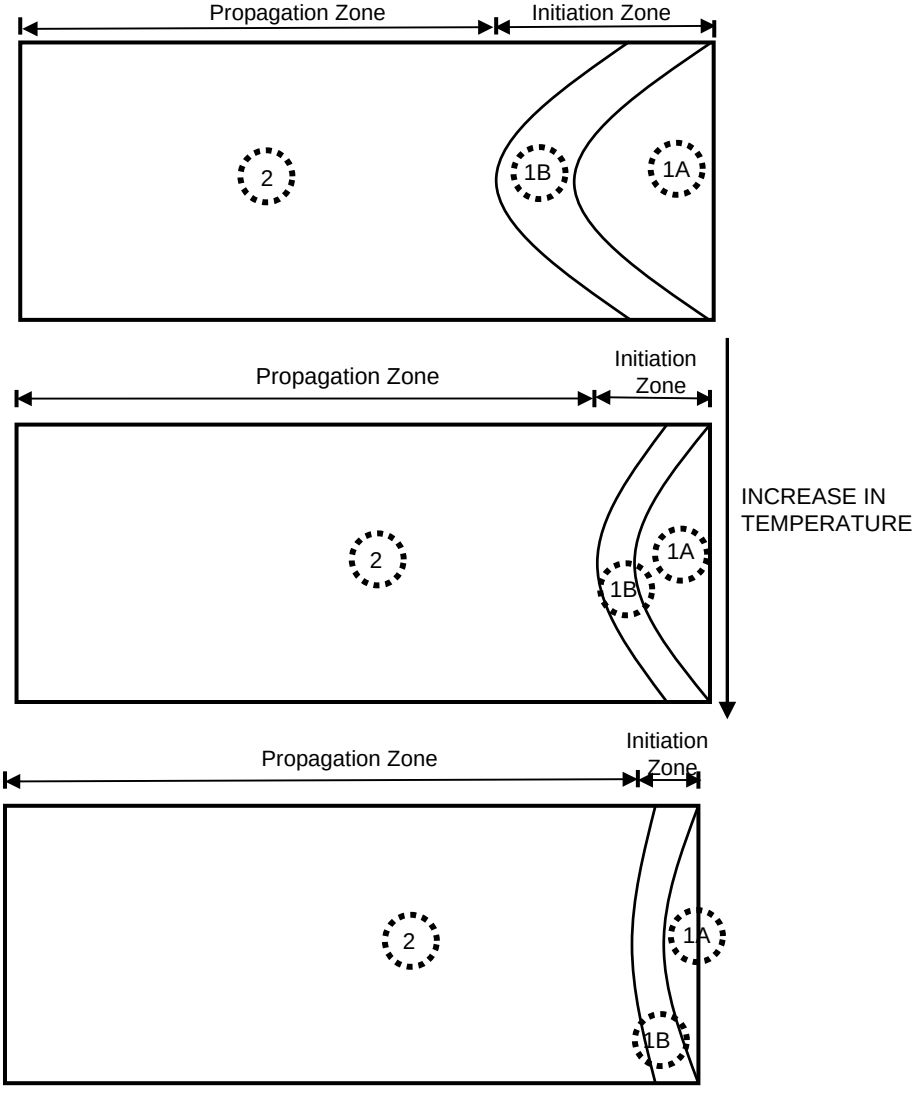

Fig. 10. Schematic of the extent of initiation and propagation zones as a function of temperature in PE–clay nanocomposite.

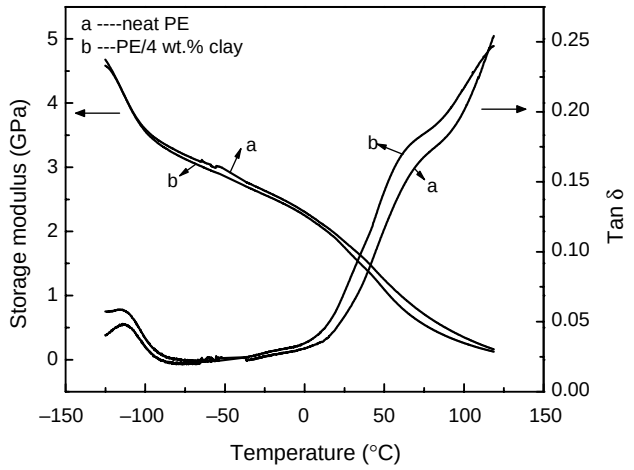

Fig. 11. Dynamic mechanical analysis plot of neat PE and PE–clay nanocomposite.

semi-crystalline polymeric materials. We will now turn our attention to structural and morphological characteristics namely, crystallinity, lamellar thickness (crystalline order), and crystal structures.

As described in Section 3.1, the reinforcement with clay increased percentage crystallinity and slightly increased lamellae thickness and the crystal structure morphology remain unaffected (Fig. 2). Previous work on neat polymers indicated that higher crystallinity and large spherulite size are detrimental to toughness [17]. Thus, the observation of higher crystallinity in the nanocomposite is expected to have a negative effect on toughness. In the light of the above, there must be other factors that have an overriding influence on impact toughness. It should be pointed out that the interfacial interaction between fillers and polymer matrix significantly influence the mechanical properties of particulate filled polymers. In our case, based on the DSC, DMA and SEM results, we believe that the interfacial interaction between nanoclay particles and polymer matrix is not adequately strong to toughen the PE–clay nanocomposite, compared with PP–clay nanocomposite system. Furthermore, the nature of the particle–matrix interface influences the toughness of filled polymer, amorphous nature of the interface is more effective to enhance the toughness of the filled polymer than that having crystalline nature of the interface. Because the more softening of the material allows for deformation to larger stains and enhances toughness. For example, Kim et al. [58] found the toughness of polyamide-12/layered silicate nanocomposites increased with the addition of nanofillers, and the interface is amorphous nature. In our case, the decrease in toughness may be also ascribed to the crystalline nature of the interface (Section 3.2, TEM analysis, Fig. 3(b2)), the growth of lamellae on the nanoclay particle surface.

4. Conclusions

1. The addition of clay to polyethylene though decreases the impact strength for the entire temperature range of Izod impact tests, however, the toughness continues to be high even at -40 °C (10 kJ/m^2).
2. Impact fracture surface of neat polyethylene and clay–reinforced polyethylene composite exhibit two primary zones: initiation and propagation zones. The fracture of polyethylene initiates with crazing, while the propagation involves a combination of different process: fast propagation of crack and shear process.
3. The fracture initiation and propagation of clay–polyethylene nanocomposite is characterized by stretching of fibrils (fibrillation) interdispersed with microvoids. The low toughness of the clay–reinforced polyethylene in relation to neat polyethylene is related to the crystal structure and interfacial interaction between the filler and the polymer matrix.
4. The reinforcement of polyethylene with nanoclay alters the primary mechanism of deformation from a combination of craze and drawing of fibrils in polyethylene to microvoid coalescence-fibrillated process.

Acknowledgements

The authors thank Mr G Zollos for provision of experimental material.

References

[1] Hadal RS, Misra RDK. Mater Sci Eng, A 2004;374:374.
[2] Hadal RS, Misra RDK. Mater Sci Eng, A 2004;380:326.
[3] Trotigon JP, Verdu J, Boissard RDe, Vallios ADe. In: Sedlaucek B, editor. Polymer composites: proceedings of prague IUPAC microsymposium on macromolecules. Berlin: De Grugter; 1985. p. 191.
[4] Dasari A, Sarang S, Misra RDK. Mater Sci Eng, A 2004;368:191.
[5] Dasari A, Rohrmann J, Misra RDK. Mater Sci Eng, A 2004;364:357.
[6] Dasari A, Misra RDK. Acta Mater 2004;52:1683.
[7] Yuan Q, Jiang W, Zhang HZ, Yin JH, An LJ, Li RKY. J Polym Sci, Part B: Polym Phys 2001;39:1855.
[8] Chan CM, Wu J, Li JX, Cheung YK. Polymer 2002;43:2981–92.
[9] Thio YS, Argon AS, Cohen RE, Weinberg M. Polymer 2002;43:3661–74.
[10] Haworth B, Raymond CL, Sutherland I. Polym Eng Sci 2001;41:1345.
[11] Albano C, Gonzalez J, Ichazo M, Rosales C, Urbina de Navarro C, Parra C. Compos Struct 2000;49:48.
[12] Wang Y, Wang JJ. Polym Eng Sci 1999;39:190.
[13] Gonzalez J, Albano C, Ichazo M, Diaz B. Eur Polym J 2002;38:2465.
[14] Price GJ, Ansari DM. Polym Int 2004;53:430.
[15] Vollenberg PHTh, Heikens D. J Mater Sci 1990;25:3089.
[16] Misra RDK, Nerlikar P, Bertrand K, Murphy D. Mater Sci Eng, A 2005;384:284.
[17] Tanniru M, Misra RDK, Bertrand K, Murphy D. Mater Sci Eng, A 2005;404:208.
[18] Tanniru M, Misra RDK. Mater Sci Eng, A 2005;405:178.
[19] Nathani H, Dasari A, Misra RDK. Acta Mater 2004;52:3217–27.
[20] Misra RDK, Nathani H, Dasari A. Mater Sci Eng, A 2004;386:175–85.
[21] La Mantia FP, Verso SL, Dintcheva NT. Macromol Mater Eng 2002;287:909–14.
[22] Messersmith PB, Giannelis EP. Chem Mater 1994;6:1719–25.
[23] Nussbaumer RJ, Caseri WR, Smith P, Tervoort T. Macromol Mater Eng 2003;288:44–9.
[24] Kornmann X, Lindberg H, Berglund LA. Polymer 2001;42:1303–10.
[25] Kornmann X, Lindberg H, Berglund LA. Polymer 2001;42:4493–9.
[26] Rong MZ, Zhang MQ, Zheng YX, Zeng HM, Walter R, Friedrich K. Polymer 2001;42:167–83.
[27] Ng CB, Ash BJ, Schadler LS, Siegel RW. Adv Compos Lett 2001;10:101.

[28] Ng CB, Schadler LS, Siegel RW. Nanostruct Mater 1999;12:507–10.
[29] Giannelis EP. Flame retardant nanocomposites materials. NIST annual conference on fire research, Gaithersburg, MD; 1998.
[30] Siegel RW, Chang SK, Ash BJ, Stone J, Ajayan PM, Doremus RW, et al. Scripta Mater 2001;44:2065–8.
[31] Okada O, Usuki A. Mater Sci Eng, C 1995;3:109–15.
[32] Wang Z, Pinnavaia TJ. Chem Mater 1998;10:1820–6.
[33] Chan CM, Wu J, Li JX, Cheng YK. Polymer 2002;43:2981–92.
[34] Giannelis EP, Krishnamoorti R, Manias E. Adv Polym Sci 1999;138: 107–47.
[35] Gilman JW, Kashiwaga T, Brown JET, Lomankin S, Giannelis EP, Manias E. Flammability studies of polymer layered silicate nanocomposites. Proceedings of the 43rd international SAMPE symposium. Part I, vol. 43; 1998. p. 1053–66.
[36] Gilman JW, Jackson CL, Morgan AB, Harris R, Manias E, Giannelis EP, et al. Chem Mater 2000;12:1866–73.
[37] Ozin GP. Adv Mater 1992;4:612–49.
[38] Alivisatos P, Barbara PF, Castleman AW, Chang J, Dixon DA, Klein ML, et al. Adv Mater 1998;10:1297–336.
[39] Mann S. Nature 1993;365:499–505.
[40] Shah D, Maiti P, Gunn E, Schmidtt DF, Jiang DD, Batt CA, et al. Adv Mater 2004;16:1173.
[41] Giannelis EP. Toughening of a brittle glassy polymer, poly(lactide-*co*-glycolide) by layered silicate nanoparticles. Private communication; 2005.
[42] Sano H, Usami T, Nakagawa H. Polymer 1998;27:1497.
[43] Wunderlich B. Macromolecular physics. New York: Academic Press; 1980 p. 58.
[44] Bassett DC. Principles of polymer morphology. London, UK: Cambridge University Press; 1981.
[45] Dasari A, Rohrmann J, Misra RDK. Polym Eng Sci 2004;44:1738.
[46] Way JL, Atkinson JR, Nutting JJ. J Mater Sci 1974;9:293.
[47] Friedrich K. Adv Polym Sci 1983;52/53:225.
[48] Ouderni M, Philips PJ. J Eng Appl Sci 1996;2:2312.
[49] Lotz B, Kovacs AJ, Wittmann JC. J Polym Sci, Polym, Phys Ed 1975;909:13.
[50] Kim GM, Michler GH. Polymer 1998;39:5689.
[51] Kim GM, Michler GH. Polymer 1998;39:5699.
[52] Pearson RA, Yee AF. J Mater Sci 1986;21:2475.
[53] Pearson RA, Yee AF. J Mater Sci 1989;24:2571.
[54] Parker DS, Sue HJ, Yee AF. Polymer 1990;31:2267.
[55] Wu JS, Mai YW. J Mater Sci 1993;28:6167.
[56] Wu JS, Yee AF, Mai YW. J Mater Sci 1994;29:4510.
[57] Wu JS, Yu DM, Mai YW, Yee AF. J Mater Sci 2000;35:307.
[58] Kim GM, Lee DH, Hoffmann B, Kressler J, Stoppelmann G. Polymer 2001;42:1095.